



HAL
open science

Enhanced magnetic properties of magneto-electrodeposited Co and Ni nanowires

Nabil Labchir, Abdelkrim Hannour, Abderrahim Ait Hssi, Didier Vincent,
Ahmed Ihlal, Mohammed Sajieddine

► **To cite this version:**

Nabil Labchir, Abdelkrim Hannour, Abderrahim Ait Hssi, Didier Vincent, Ahmed Ihlal, et al.. Enhanced magnetic properties of magneto-electrodeposited Co and Ni nanowires. *Current Applied Physics*, 2021, 25, pp.33-40. 10.1016/j.cap.2021.02.010 . ujm-03268960

HAL Id: ujm-03268960

<https://ujm.hal.science/ujm-03268960>

Submitted on 10 Mar 2023

HAL is a multi-disciplinary open access archive for the deposit and dissemination of scientific research documents, whether they are published or not. The documents may come from teaching and research institutions in France or abroad, or from public or private research centers.

L'archive ouverte pluridisciplinaire **HAL**, est destinée au dépôt et à la diffusion de documents scientifiques de niveau recherche, publiés ou non, émanant des établissements d'enseignement et de recherche français ou étrangers, des laboratoires publics ou privés.



Distributed under a Creative Commons Attribution - NonCommercial 4.0 International License

Enhanced magnetic properties of magneto-electrodeposited Co and Ni nanowires

Nabil Labchir^{a,b*}, Abdelkrim Hannour^b, Abderrahim Ait hssi^b, Didier Vincent^a, Ahmed Ihlal^b, Mohammed Sajieddine^c

^aUniv Lyon, UJM-Saint-Etienne, CNRS, LabHC, UMR 5516, F-4203, Saint-Étienne, France

^bUniv Ibn Zohr, Faculty of Sciences Agadir, LabMER, BP 8106, 80000, Agadir, Morocco

^cUniv Sultan Moulay Slimane, FST, LabPM, BP 523, 23000, Beni Mellal, Morocco

* Corresponding author: nabil.labchir@univ-st-etienne.fr

Abstract:

The present paper examines the influence of an applied magnetic field B (AMF B) on the **physical and chemical properties** of electrodeposited Cobalt (Co) and Nickel (Ni) nanowires into anodic aluminum oxide (AAO) membranes. The deposition potential and the effect of the AMF B on the mass transport rate of Ni and Co ions to the bottom of the pores were examined using cyclic voltammetry (CV) and current density–time curves. X-ray diffraction (XRD) studies show that the AMF B promotes the growth of Co and Ni into the membrane pores. The AMF B effect on the morphology and chemical composition of the electrodeposited nanowires were studied by scanning electron microscopy (SEM) and energy dispersive X-ray spectroscopy (EDXS), respectively. Co nanowires exhibit a high coercive field H_c , shape anisotropy, and squareness ratio $\frac{M}{M_s}$ than those corresponding to Ni nanowires.

Keywords: Co and Ni nanowires; electrodeposition; magnetic field; AAO membrane; magnetic properties.

1. Introduction

The fabrication of ferromagnetic materials with nanometric scale and the study of their **physical and chemical** properties have recently attracted a great technological and scientific interest. Currently, Co and Ni nanowires have garnered considerable attention due to their potential applications including, for example, the energy storage systems [1,2], magnetic and optical media [3,4], sensors [5-8], spintronics [9,10] and heterogeneous catalysis [11,12]. In the magnetic applications, the anisotropy of Co and Ni nanowires has improved performances compared to the bulk material. The shape anisotropy of nanowires can become dominant when they have weak magnetocrystalline anisotropy. This sparked interest to develop a protocol for the synthesis of ferromagnetic nanowires with controlled size because the magnetic properties are strongly depending on the particle size, shape and orientation. Membrane technology is known as a promising technique for making nanowires with significant anisotropy [13]. Several works [14,15] have confirmed that the growth of nanomaterials in a nanoporous membrane improves the magnetic behavior compared to that of a bulk material or a thin film. The electrochemical growth configured as an alternative, economically affordable, environmental and competitive method to synthesize Co and Ni nanowires. In this technique, we can control the growth **nature of the nanomaterials and** the nanowires length by acting on the electrodeposition time that responds to the choice of the deposition potential [16].

Moreover, many works have been devoted to studying **the physical and chemical** properties of the ferromagnetic nanowires by the magneto-hydrodynamic effect (MHD), generated by the presence of the AMF B during the electrochemical deposition [17,18]. However, **in the electrolytic deposition, the disordered active surface** induced a thermodynamic potential thus provides a microstructural transformation of growth on the substrate in relation with the magnetization [19]. Indeed, Ganesh et al. [20] reported on their work the AMF B effect on Ni electrodeposition from nickel sulfate and nickel chloride bath. They have revealed that the increase of the microroughness of Ni deposit decreases the overpotential during the electrochemical reduction of Ni. Moreover, **the crystallites deposited electrochemically** under AMF B are very fine unlike those deposited in the absence of an AMF B. In their work, Bund et al. [21] have deposited Ni films from nickel sulfate medium with an AMF B up to 0.7 T. They reported that under a constant and homogenous AMF B, uniform and compact deposits were obtained with smaller Ni grains. Within this context, Zieliński et al [22] investigated the effects of constant magnetic field of 1.2 T on the

electrochemical growth of cobalt alloys at constant potential from sulfate bath. They observed that the Co alloys deposited with AMF B exhibit a dense and smoother surface, reduced fractures, and smaller Co grains.

However, many properties of ferromagnetic nanowires synthesized by this technique of electrodeposition still have not been studied completely and this has motivated researchers in magnetism of nanomaterials to focus on this area. Therefore, the main objective of our study is to examine the effect of a perpendicular AMF B to the working electrode on the electrochemical deposition of Co and Ni nanowires and more particularly on their magnetic properties such as anisotropy, coercivity and magnetization.

The present work was performed to exploit X-ray diffraction (XRD), scanning electron microscopy (SEM) and SQUID analysis in order to reveal how the electrochemical growth of Co and Ni nanowires into AAO membranes depends on the AMF B.

2. Experimental

2.1 Synthesis of nanowires

AAO membranes (Whatman Anodisc) having 60 μm in thickness, uniform pore density of 10^9 pore/ cm^2 with an average pore diameter of 100 nm (**Fig. 1**), were used for nanowires growth. The electrochemical reduction of Co and Ni ions was carried out into AAO membrane pores using a standard potentiostat system (PGZ 301 & voltamaster 4) of three-electrodes. To facilitate the electrodeposition, one back side of the porous membrane was coated with 3 μm of copper (Cu) by rf sputtering technique, which acted as working electrode. Ag/AgCl and platinum sheet were used in all growth experiments as reference and counter electrodes, respectively. Two different aqueous solutions containing 2.5 g of nickel sulfate hexahydrate ($\text{NiSO}_4 \cdot 6\text{H}_2\text{O}$, 99.9 %, Sigma Aldrich), 2.5 g of nickel chloride hexahydrate ($\text{NiCl}_2 \cdot 6\text{H}_2\text{O}$, 99.9 %, Sigma Aldrich) and 2.5 g of cobalt sulfate hexahydrate ($\text{CoSO}_4 \cdot 6\text{H}_2\text{O}$, 99.9 %, Sigma Aldrich), 2.5 g of cobalt chloride hexahydrate ($\text{CoCl}_2 \cdot 6\text{H}_2\text{O}$, 99.9 %, Sigma Aldrich) were used to reduce electrochemically Ni and Co ions, respectively. 3 g of boric acid (H_3BO_3 , 99 %, Sigma Aldrich) was added to each solution as a precursor to stabilize the pH close to 3.4 at the electrode-solution interface. The species used in the electrodeposition experiments were of analytical grade. As displayed in **Fig. 2**, the electrochemical deposition of Co and Ni nanowires was performed with presence of an homogenous AMF B perpendicular to the nanoporous membranes up to 0.5 T, which generated by a commercial NdFeB permanent magnet. The applied potential in all

electrodeposition experiments was kept in all experiments at -1 V. High data reproducibility is observed for all growth and characterization experiments of Co and Ni nanowires.

Fig. 1 (Here)

Fig. 2 (Here)

2.2 Characterization materials

XRD spectra was determined using X'Pert *PRO* diffractometer in the angular range 16-80° with a step scanning of 0.03° operating with CuK α radiation ($\lambda = 1.5406 \text{ \AA}$) and 20 kV in voltage acceleration. The morphological properties of Co and Ni nanowires were recorded using scanning electron microscope (Quanta 200-FEI SEM), coupled with energy-dispersive X-ray detector in order to study the AMF B effect on the average atomic composition of Co and Ni metals. Superconducting Quantum Interference Device (SQUID) magnetometer were used to investigate the magnetic measurements, such as coercive field H_c , squareness ratio $\frac{M}{M_s}$ and magnetization M .

3. Results and Discussion

3.1 Electrochemical investigations

The CV curves are recorded in order to study the AMF B effect on the specific contribution of different species (Ni, Co) in the aqueous solutions. **Fig. 3** presents **the CV curves** for a solution containing Co ions at room temperature. The voltammograms show that at constant potential, the oxidation current density of Co is less important for $B = 0 \text{ T}$. Moreover, when the AMF B was imposed during the electrochemical scanning, we observed that the peak of the oxidation current density of the deposit at pH 3.4 appeared more important and shifted from -0.3 to -0.23 V. This is related to the increase of the current density of deposit dissolution due to the thickness reduction of the double charging layer, which is explained by the effect of the Lorentz force generated by the AMF B on the motion of Ni ions into the solution [23]. In addition, the **results clearly indicate the** low enhancement in Co reduction current density and a plateau of Co reduction potentials that starts from -0.9

up to -1.1 V. The presence of a cathodic peak at -0.7 V is assigned to the electrochemical reduction potential of H^+/H_2 .

Fig. 3 (Here)

Figure 4 presents the evolution of the current density deposition of Ni as a function of potential in the AAO membranes.

Fig. 4 (Here)

As shown in the CV curves, the AMF B increases slightly the resulting current density according to the same explanation reported for Ni growth. From the cathodic zone, the reduction and nucleation of the Ni start at -0.85 V and can reach -1.1 V, above this potential, a fast increase of the resulting current density produced from the strong evolution of hydrogen at the electrodeposition of Ni is observed. Note also that the oxidation peak in the anodic part is more pronounced. This is due to the oxidation of the deposited Ni film.

The CV results obtained for Ni and Co confirm that the AMF B is an important parameter that must be taken into account for the deposition experiments. As an interesting result from these electrochemical studies, the suitable potential to electrochemically deposit Ni and Co nanowires is -1.1 V. The choice of this potential is justified by the fact that the hydrogen bubbles are not appearing on the AAO membrane surface. On the other hand, the other applied potentials showed a very important quantity of hydrogen bubbles which presents undesirable parasites for a successful deposit.

Fig. 5 shows the variation of the deposition current density of Ni and Co ions into AAO membrane pores as a function of time with and without presence of AMF B (0.5 T) at constant applied potential of -1.1 V vs Ag/AgCl.

Fig. 5 (Here)

From **Fig. 5**, it can be observed that the curves of the electrochemical growth evolution for Ni and Co nanowires during the 40 min showed an enhancement in the diffusion-limiting current density with the presence of an AMF B. More precisely, it is caused by the thickness reduction of the double charging layer, which comes from the hydrodynamic flow variation via the magnetohydrodynamic effect (Lorentz force). In addition, one could also explain the increase of the current density with the rate increase of the transferred ions towards the bottom of the membrane pores by the appearance of a concentration gradient $\vec{\nabla}c$ force of the magnetic ions that can be expressed by the following formula [24] :

$$\vec{F}_p = \frac{\chi_m B^2 \vec{\nabla} c}{2\mu_0} \quad (1)$$

where χ_m is the molar susceptibility of ions and μ_0 is the permeability of free space ($4\pi \times 10^{-7} \text{ T} \cdot \text{mA}^{-1}$).

As reported elsewhere [25,26], the limiting current increases with the magnetic field during the reduction and the diffusion of Ni and Co ions according to the law $I \approx B^{1/3}$, which confirms the showed enhancement of the current density in our work.

3.2 Microstructural, morphological and composition analysis

Diffraction studies were carried out in order to investigate the effect of the AMF B on the crystalline structure of Ni and Co nanowires. **Figure 6a-b** display two typical X-ray diffraction spectrum for Ni and Co nanowire arrays embedded into AAO membranes with and without an AMF B.

Fig. 6 (Here)

As shown in **Fig. 6a**, the electrodeposited Ni nanowires present a face-centered cubic (fcc) structure (JCPDS n° 04-0850). The growth under the AMF B makes the (111) and (200) peaks more intense and causes the birth of a new crystallographic peak (111) in the XRD spectrum. On the other hand, the electrodeposited Co nanowires present a hexagonal-close-packed (hcp) structure (JCPDS n° 89-7093).

As shown in **Fig. 6b**, the XRD spectrum revealed that the nanowires deposited under AMF B have strong intensities for (100), (002) and (110) peaks. We also observe the presence of some peaks of alumina substrate. It was known that during the electrochemical growth of Ni and Co nanowires, as a highly inhibited process, the appearance of the reflection (200) for Ni and the intensity increase of (110) reflection for Co are affected by the chemical species such as hydrogen ions, nickel or cobalt hydroxide [27].

Therefore, the AMF B improves the hydrogen evolution reaction that increases the specific adsorption of dyroxides or oxyhydroxide species [28,29]. Furthermore, the magneto-hydrodynamic effect is an additional convection induced by the Lorentz force on the solution

during the electrochemical reduction of Ni and Co ions. This effect generates an enhancement of hydrogen evolution and can be invoked to be responsible for the texture changes on Ni and Co nanowires growth [30].

To approximately evaluate the grain size of Ni and Co deposits from their higher intense reflections (111) and (100), respectively, we have used the Scherrer formula [31]:

$$D = \frac{0.9K}{\delta_{cor} \cos \theta} \quad (2)$$

where K is the wavelength of X-ray beam, δ_{cor} is the corrected FWHM of the XRD peak (optimized by FullProf software), and θ is the Bragg's angle. It should be noted that the grain size has been qualitatively approached with an approximate error of ± 0.15 . The repeated calculations have shown that the AMF B decreases the grain size from 35.12, 30.04 nm to 29.52, 26.68 nm for Co and Ni, respectively. Our results are in good agreement with those reported previously [32-35].

The morphology of the Co and Ni nanowire arrays was investigated by SEM analysis as displayed in Fig. 7.

Fig. 7 (Here)

After a chemically attack process of the copper which acts as the cathode by iron perchloride solution, and a dissolution of the samples in 1M of NaOH to partially remove the alumina of the AAO membrane, the samples become ready for the SEM analysis, in order to clearly observe the nanowires. From the SEM images, the nanowires are filled approximately 100% by Ni and Co elements as showing in Fig.7a, b and c, d, respectively. It is possible to observe that the Co and Ni nanowires incorporated in the AAO membranes have a diameter of 100 nm and a mean inter-interface spacing of 100 nm.

Fig. 8 illustrates the elementary composition of the grown Co and Ni nanowires.

Fig. 8 (Here)

As shown in the spectra, the purities of Co and Ni nanowires are greatly confirmed by EDXS analysis, which indicates no presence of other impurities in the synthesized nanowires. The peaks corresponding to Al and O arise from the used AAO membranes for nanowires

electrodeposition. Moreover, based on the EDXS measurements (see tables) collected for each spectrum, it is noted that when imposing the AMF B during the electrochemical growth process, the atomic averages of Co and Ni elements shifted qualitatively from 47 %, 32 % to 56 %, 51 %, respectively. The showing enhancement in the atomic ratio is justified by the birth of the magnetohydrodynamic effect, which considered as the most responsible for increasing the speed of ions migration during the reduction process. Consequently, an increase in the transferred amount towards the bottom of pores is observed during the total pore filling by Co and Ni metals.

3.3 Magnetic properties

The effect of the external AMF B on the magnetic properties during the electrodeposition of Co and Ni nanowire arrays is investigated by the hysteresis loops measurements. During the measurements, the external magnetic field was applied perpendicular and parallel to the nanowires electrodeposited with and without presence of an AMF B.

Fig. 9 presents the room-temperature hysteresis loops of Ni and Co nanowires electrodeposited without (**Fig. 9a-c**) and with (**Fig. 9b-d**) an AMF B.

Fig. 9 (Here)

From **Fig. 9**, the presence of AMF B during the electrochemical growth of the samples does not change the direction of the easy axis of magnetization, which always remains oriented along the wire axis for Co and Ni. This result corroborates the previous findings reported by Barriga et al. [36] and Cho et al. [37].

Table 1 displays the variation of the squareness ratio $\frac{M}{M_s}$ (SQ) and the coercive field H_c versus applied magnetic field.

Table 1 (Here)

The presence of an AMF B shows significant influence on the magnetic properties of Co and Ni nanowire arrays (table 1). Indeed, the AMF B enhances the SQ and H_c in both directions (parallel and perpendicular) of Co and Ni nanowires (NWs). This effect of the AMF B is more pronounced for Co nanowires, where SQ and H_c are enhanced from 0.43, 1430 Oe to 0.51, 2700 Oe, respectively. The X-ray spectra of electrodeposited Co and Ni samples reveal that the AMF B changes the crystalline micro-structure by increasing the intensities of the reflections peaks. Several researchers [36, 37, 38, 39] reported that the presence of the AMF

B during the electrochemical growth can alter the growth of Co nanowires and also promotes the c-axis alignment of Co nanowires to follow its direction, which can affect the magnetic properties. Moreover, during the electrochemical growth, the AMF B affect locally the growth mechanisms by the size reduction of Ni and Co grains as revealed in our work and also the modification of the location of the magnetic atoms in each crystal structure. These mentioned factors can be considered as responsible for a local creation of the mono-domains from crystallites. Therefore, the increase of SQ and H_c could be explained by a possible dominance and enhancement of the shape anisotropy of Ni and Co crystals within the pores of the AAO membranes.

Moreover, from the hysteresis cycles we can qualitatively deduce the magnetic anisotropy field H_a . Its value is determined by the convergence point of the two hysteresis cycles in both scan directions. The measurements reveal a value of 12 kOe for Co nanowires, this value is slightly higher than the magnetic shape anisotropy (9 kOe). The high measured value for H_a can be explained by the textures along the long axis of the nanowires, which can be guessed from X-ray diffraction. Indeed, the anisotropy field of the nickel wires (12 kOe) exceeds the magnetic shape anisotropy (3 kOe) [40,41]. This is explained by a possible magnetocrystalline anisotropy induced by the presence of the magnetic field via the orientation of a magnetic moment density in a defined direction. This orientation compensates the dipolar interactions and makes the nanowires behave like a partially hard material.

Fig. 10 displays the measurements of the variation of moments dynamic as a function of temperature for Co and Ni nanowires.

Fig. 10 (Here)

The measurement process starts with the cooling of the sample to a temperature of (5 K) without any applied magnetic field, after which the $M(T)$ curve is recorded by slow heating of the sample up to 300 K in the presence of a magnetic field of 10 kOe, applied parallel to the wire. This study allowed us to perform at low temperature a comparison between the inversion process generated by the field and that of thermal demagnetization. The $M(T)$ curves show a shifting of the magnetization from a maximum value to another lower value with a magnetization change order of about 1.2 at a temperature of 30 K during the first stage

of heating for Co (**Fig. 10a**) and Ni (**Fig. 10b**) nanowires electrodeposited with and without presence of AMF B. The crystals are ferromagnetic at low temperature and at room temperature (300 K) as observed in hysteresis cycles. Indeed, it is possible that the dipolar interaction between adjacent nanowires is responsible for such a magnetization switching observed in parallel field measurements. In addition, the shape anisotropy can affect the magnetization switching in terms of reduced grain size for the magnetically prepared samples [42]. Finally, the $M(T)$ curves nature observed in our work describe such a cooperative switching phenomenon, thus confirming the dominance of the higher shape anisotropy inside the magneto-electrodeposited Ni and Co nanowires.

4. Conclusion

Oriented Co and Ni nanowire arrays have been successfully prepared by electrodeposition method under AMF B control into AAO membranes. The mobility of ions assisted electrochemical growth responsible for nanowire formation was enhanced with the presence of AMF B for both Co and Ni nanowires. XRD analysis emphasized the growth of Co and Ni nanowires. Scherrer calculations revealed a decreasing in the grain size for Co and Ni nanowires. EDXS investigations have reported an enhancement on the average atomic ratio resulting from the magnetohydrodynamic effect during the growth of Co and Ni nanowires. A high squareness ratio (SQ), coercitive field H_c and magnetization values are reached in the parallel direction for the magneto-electrodeposited nanowires, which indicates the modification of the shape anisotropy and the dipolar interaction into Co and Ni nanowires. The present results can be qualified the magneto-electrodeposition as a general mechanism that offers the possibility of growing and controlling the magnetic proprieties of one-dimensional structures. Thus, the highly textured Ni and Co nanowires prepared here are promising candidates for recording, coaxial multifunctional nanostructures and other multifunctional devices.

Declaration of competing interests

The authors of this paper declare that they have no known competing financial interests or personal relationships that could have appeared.

Acknowledgment

The authors acknowledge the financial support from PHC-Toubkal Project (PHC TBK/85/17)
- N° Campus France: 38983UH.

References

- [1] L. Zhan, S. Wang, L. X. Ding, Z. Li, H. Wang, Binder-free Co–CoO_x nanowire arrays for lithium ion batteries with excellent rate capability and ultra-long cycle life, *J. Mater. Chem.* 3 (2015) 19711-19717.
- [2] C. Xu, J. Liao, C. Yang, R. Wang, D. Wu, P. Zou, C. P. Wong, An ultrafast, high capacity and superior longevity Ni/Zn battery constructed on nickel nanowire array film, *Nano. Energy.* 30 (2016) 900-908.
- [3] A. S. Samardak, E. V. Sukovatitsina, A. V. Ognev, L. A. Chebotkevich, R. Mahmoodi, S. M. Peighambari, F. Nasirpouri, High-density nickel nanowire arrays for data storage applications, *J. Phys. Conf.* 345 (2012) 012011.
- [4] S. Z. Chu, S. Inoue, K. Wada, K. Kurashima, Fabrication of integrated arrays of ultrahigh density magnetic nanowires on glass by anodization and electrodeposition, *Electrochim. Acta.* 51 (5) (2005) 820-826.
- [5] S. Wang, K. Chen, M. Wang, H. Li, G. Chen, J. Liu, S. Liu, Controllable synthesis of nickel nanowires and its application in high sensitivity, stretchable strain sensor for body motion sensing, *J. Mater. Chem. C.* 6 (17) (2018) 4737-4745.
- [6] P. D. McGary, L. Tan, J. Zou, B. J. Stadler, P. R Downey, A. B. Flatau, Magnetic nanowires for acoustic sensors, *J. Appl. Phys.* 99 (8) (2006) 08B310.
- [7] F. Xie, X. Cao, F. Qu, A. M. Asiri, X. Sun, Cobalt nitride nanowire array as an efficient electrochemical sensor for glucose and H₂O₂ detection, *Sens. Actuator B-Chem.* 255 (2018) 1254-1261.
- [8] J. Tian, N. Cheng, Q. Liu, W. Xing, X. Sun, Cobalt phosphide nanowires: efficient nanostructures for fluorescence sensing of biomolecules and photocatalytic evolution of dihydrogen from water under visible light, *Angew. Chem. Int. Ed. (international).* 54 (18) (2015) 5493-5497.
- [9] S. Pramanik, C. G. Stefanita, S. Patibandla, S. Bandyopadhyay, K. Garre, N. Harth, M. Cahay, Observation of extremely long spin relaxation times in an organic nanowire spin valve, *Nat. Nanotechnol.* 2 (4) (2007) 216.
- [10] C. Tannous, A. Ghaddar, J. Gieraltowski, Nanowire arrays, surface anisotropy, magnetoelastic effects and spintronics, *Appl. Phys. Lett.* 100 (18) (2012) 182401.
- [11] Y. Zhang, B. Ouyang, J. Xu, G. Jia, S. Chen, R. S. Rawat, H. J. Fan, Rapid synthesis of cobalt nitride nanowires: highly efficient and low-cost catalysts for oxygen evolution., *Angew. Chem. Int. Ed. (international).* 55 (30) (2016) 8670-8674.
- [12] W. Yan, D. Wang, L. A. Diaz, G. G. Botte, Nickel nanowires as effective catalysts for urea electro-oxidation, *Electrochim. Acta.* 134 (2014) 266-271.
- [13] N. Labchir, A. Hannour, D. Vincent, A. Ihlal, M. Sajieddine, Magnetic field effect on electrodeposition of CoFe₂O₄ nanowires, *Appl. Phys. A.* 125 (2019) 748.

- [14] P. L. Cavallotti, A. Vicenzo, M. Bestetti, S. Franz, Microelectrodeposition of cobalt and cobalt alloys for magnetic layers, *Surf. Coat. Technol.* 73 (2003) 169-70.
- [15] N. Labchir, A. Hannour, D. Vincent, A. A. Hssi, A. Ihlal, M. Sajieddine, Magneto-electrodeposition of granular Co–Cu nanowire arrays. *Mater. Res. Express.* 6 (2019) 1150c3.
- [16] N. Labchir, A. Hannour, D. Vincent, A. A. Hssi, M. Ouafi, K. Abouabassi, A. Ihlal, M. Sajieddine, (2020). Tailoring the optical bandgap of pulse electrodeposited CoFe_2O_4 thin films, *J. Electron. Mater.* <https://doi.org/10.1007/s11664-019-07923-y>.
- [17] J. A. Koza, F. Karnbach, M. Uhlemann, J. McCord, C. Mickel, A. Gebert, S. Baunack, L. Schultz, Electrocrystallisation of CoFe alloys under the influence of external homogeneous magnetic fields—Properties of deposited thin films, *Electrochim. Acta.* 55 (2010) 819-31.
- [18] V. Georgescu, M. Daub, Magnetic field effects on surface morphology and magnetic properties of Co-Ni-P films prepared by electrodeposition, *Surf. Sci.* 60 (2006) 4195-9
- [19] G. Hibbard, U. Erb, K.T. Aus, U. Klement, G. Palumbo, Thermal stability of nanostructured electrodeposits, *Mater. Sci. Forum.* 386-388 (2002) 387-96.
- [20] V. Ganesh, D. Vijayaraghavan, V. Lakshminarayanan, Fine grain growth of nickel electrodeposit: effect of applied magnetic field during deposition, *Appl. Surf.Sci.* 240 (1-4) (2005) 286–295.
- [21] A. Bund, A. Ispas, G. Mutschke Magnetic field effects on electrochemical metal depositions, *Sci. Technol. Adv. Mater.* 9 (2) (2008) 024208.
- [22] M. Zieliński, Influence of constant magnetic field on the electrodeposition of cobalt and cobalt alloys, *Int. J. Electrochem. Sci.* 8 (11) (2013) 12192–12204.
- [23] P. C. Mondal, C. Fontanesi, D. H. Waldeck, R. Naaman, Field and chirality effects on electrochemical charge transfer rates: spin dependent electrochemistry, *ACS. Nano.* 9 (3) (2015) 3377-3384.
- [24] O. Lioubashevski, E. Katz, I. Willner, Magnetic field effects on electrochemical processes: a theoretical hydrodynamic model, *J. Phys. Chem. B.* 108 (18) (2004) 5778-5784.
- [25] O. Aaboubi, A.Y. Ali- Omar, A. Franczak, K. Msellak, Investigation of the electrodeposition kinetics of Ni–Mo alloys in the presence of magnetic field, *J. Electroanal. Chem.* 737 (2015) 226–234.
- [26] J. M. D. Coey, G.Hinds, Magnetic electrodeposition. *J. Alloy. Compd.* 326(1-2) (2001) 238-245.
- [27] K. C. Chan, N. S. Qu, D. Zhu, Quantitative texture analysis in pulse reverse current electroforming of nickel. *Surface and Coatings Technology*, 99 (1-2) (1998) 69-73.
- [28] A. Ispas, H. Matsushima, W. Plieth, A. Bund, Influence of a magnetic field on the electrodeposition of nickel–iron alloys, *Electrochimica. Acta.* 52 (8) (2007) 2785-2795.
- [29] N. Labchir, A. Hannour, D. Vincent, D. Jamon, J. Y. Michalon, A. Ihlal, M. Sajieddine, Spontaneous Faraday rotation of $\text{Co}_x\text{Fe}_{3-x}\text{O}_4$ thin films electrodeposited under a static magnetic field. *J. Mater Sci: Mater. Electron* (2020). <https://doi.org/10.1007/s10854-020-03652-9>.
- [30] H. Matsushima, T. Nohira, I. Mogi, Y. Ito, Effects of magnetic fields on iron electrodeposition. *Surface and Coatings Technology*, 179(2-3) (2004) 245-251.
- [31] N. Labchir, E. Amaterz, A. Hannour, A. A. Hssi, D. Vincent, A. Ihlal, M. Sajieddine, (2019). Highly efficient nanostructured CoFe_2O_4 thin film electrodes for electrochemical degradation of rhodamine B, *Water. Environ. Res.* <https://doi.org/10.1002/wer.1272>.

- [32] C. Wang, Y. B. Zhong, J. Wang, Z. Q. Wang, W. L. Ren, Z. S. Lei, Z. M. Ren, Effect of magnetic field on electroplating Ni/nano-Al₂O₃ composite coating, *J. Electroanal. Chem.* 630 (1-2) (2009) 42-48.
- [33] J. Y. Chen, H. R. Liu, N. Ahmad, Y. L. Li, Z. Y. Chen, W. P. Zhou, X. F. Han, Effect of external magnetic field on magnetic properties of Co–Pt nanotubes and nanowires, *J. Appl. Phys.* 109 (7) (2011) 07E157.
- [34] H. Pan, B. Liu, J. Yi, C. Poh S. Lim, J. Ding, J. Lin, Growth of single-crystalline Ni and Co nanowires via electrochemical deposition and their magnetic properties, *J. Phys. Chem. B.* 109 (8) (2005) 3094-3098.
- [35] D. Li, A. Levesque, A. Franczak, Q. Wang, J. He, J. P. Chopart, Evolution of morphology in electrodeposited nanocrystalline Co–Ni films by in-situ high magnetic field application, *Talanta.* 110 (2013) 66-70.
- [36] J. U. Cho, J. H. Wu, J. H. Min, J. H. Lee, H. L. Liu, Y. K. Kim, Effect of field deposition and pore size on Co/Cu barcode nanowires by electrodeposition, *J. Magn. Mater.* 310 (2) (2007) 2420-2422.
- [37] J. Sanchez-Barriga, M. Lucas, G. Rivero, P. Marin, A. Hernando, Magneto-electrolysis of Conanowire arrays grown in a track-etched polycarbonate membrane, *J. Magn. Mater.* 312 (1) (2007) 99-106.
- [38] S. Ge, C. Li, X. Ma, W. Li, L. Xi, C. X. Li, Approach to fabricating Co nanowire arrays with perpendicular anisotropy: application of a magnetic field during deposition, *J. Appl. Phys.* 90 (1) (2001) 509-511.
- [39] N. Labchir, A. Hannour, A. A. Hssi, D. Vincent, K. Abouabassi, A. Ihlal, M. Sajieddine . Synthesis and characterization of CoFe₂O₄ thin films for solar absorber application, *Mater Sci. Semicond. Process.* 111 (2020) 104992.
- [40] A. S. Samardak, A. V. Ognev, A. Y. Samardak, E. V. Steblyy, E. B. Modin, L. A. Chebotkevich, F. Nasirpouri, Variation of magnetic anisotropy and temperature-dependent FORC probing of compositionally tuned Co-Ni alloy nanowires. *Journal of Alloys and Compounds*, 732 (2018) 683-693.
- [41] A. S. Samardak, F. Nasirpouri, M. Nadi, E. V. Sukovatitsina, A. V. Ognev, L. A. Chebotkevich, S. V. Komogortsev, Conversion of magnetic anisotropy in electrodeposited Co–Ni alloy nanowires, *J. Magn. Mater.* 383 (2015) 94-99.
- [42] K. Maaz, S. Karim, M. Usman, A. Mumtaz, J. Liu, J. L. Duan, M. Maqbool, Effect of crystallographic texture on magnetic characteristics of cobalt nanowires. *Nanoscale. Res. Lett.* 5 (7) (2010) 1111.

Figure captions:

Fig. 1 SEM images of AAO membranes. a) Top view, b) Cross sectional view.

Fig. 2 Experimental setup used for the electrochemical growth of Co and Ni nanowires.

Fig. 3 Cyclic voltammetry for an aqueous solution of 2 g CoSO₄ + 2 g CoCl₂. Sweep rate: 20 mV/s.

Fig. 4 Cyclic voltammetry for an aqueous solution of 2 g NiSO₄ + 2 g NiCl₂. Sweep rate: 20 mV/s.

Fig. 5 Current density–time transients recorded with and without AMF B during Ni and Co nanowires growth.

Fig. 6 XRD patterns of electrochemically grown nanowires in AAO templates. (a) Ni nanowires, (b) Co nanowires.

Fig. 7 SEM images of deposited Co and Ni nanowires with (a, c) and without (b, d) presence of an AMF B.

Fig. 8 EDXS spectra for Ni (a) and Co (b) nanowires embedded in AAO membranes.

Fig. 9 Measured hysteresis loops of Ni (a, b) and Co (c, d) nanowires at room temperature.

Fig. 10 M (T) curves for Co (a) and Ni (b) nanowires electrodeposited with and without an AMF B (B_{app}).

Table captions

Table 1. Magnetic parameters of deposited Co and Ni nanowires.

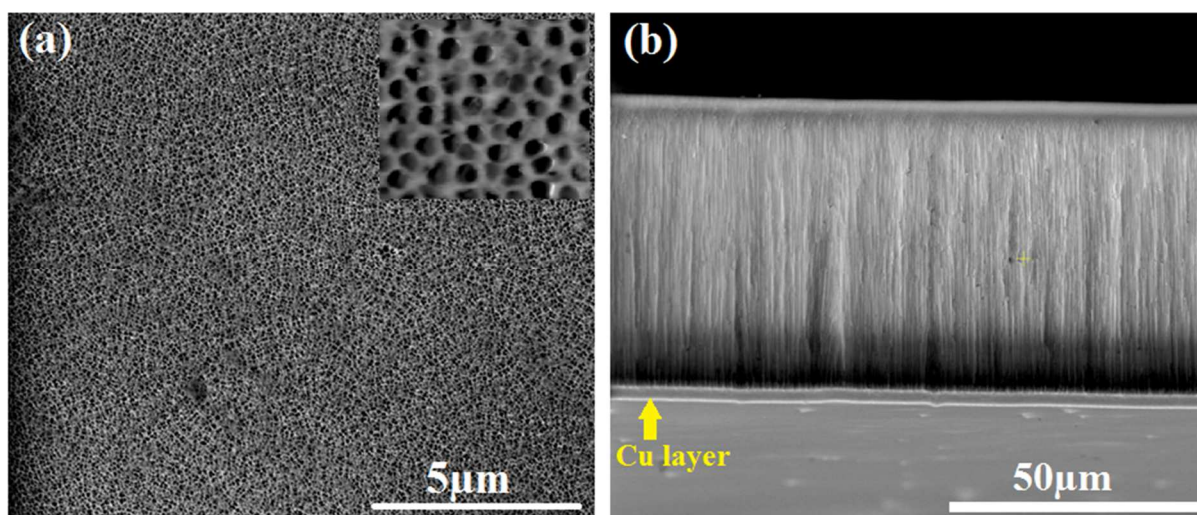


Fig. 1

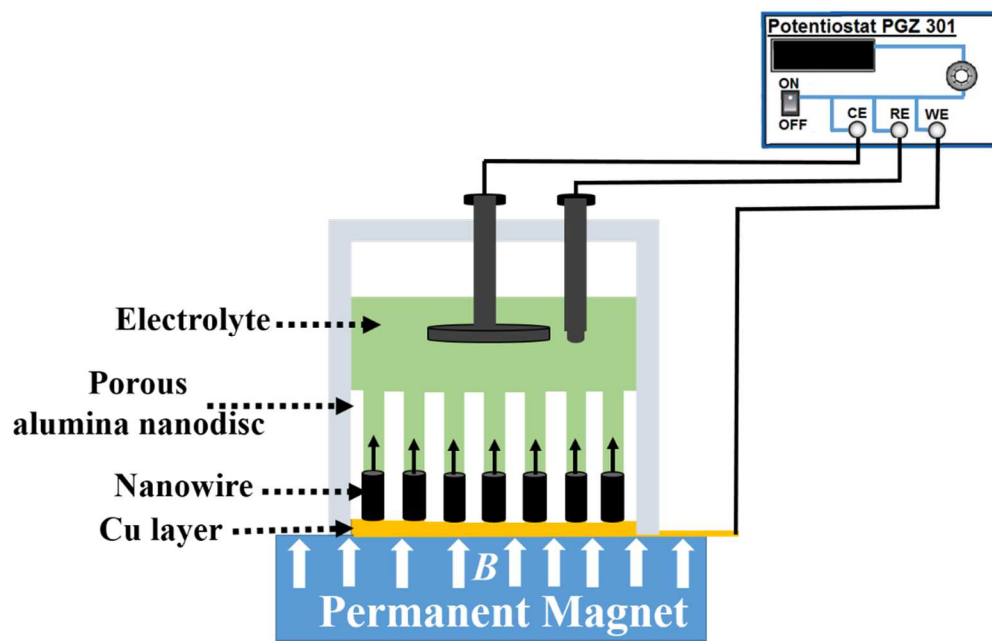


Fig. 2

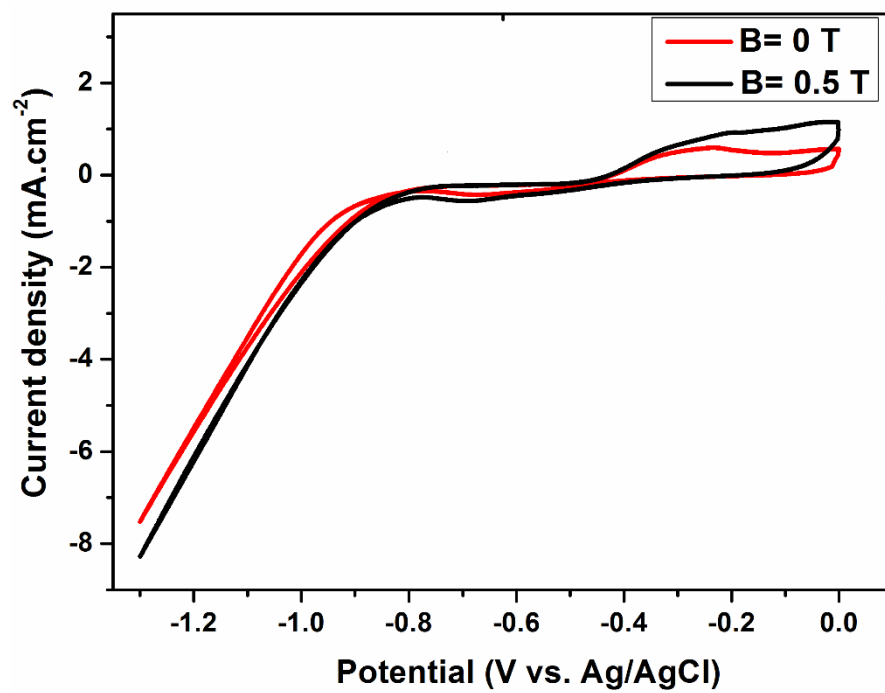


Fig. 3

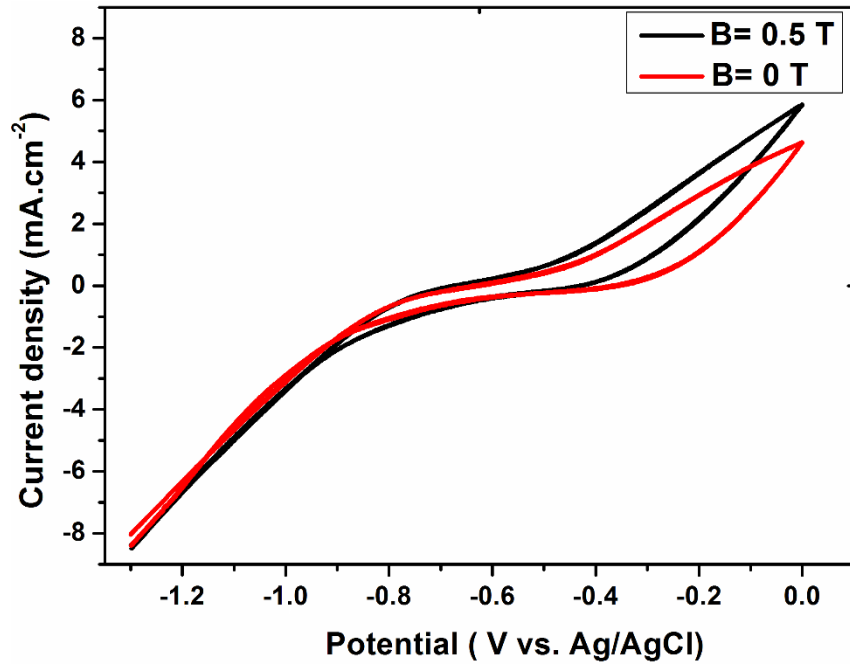


Fig. 4

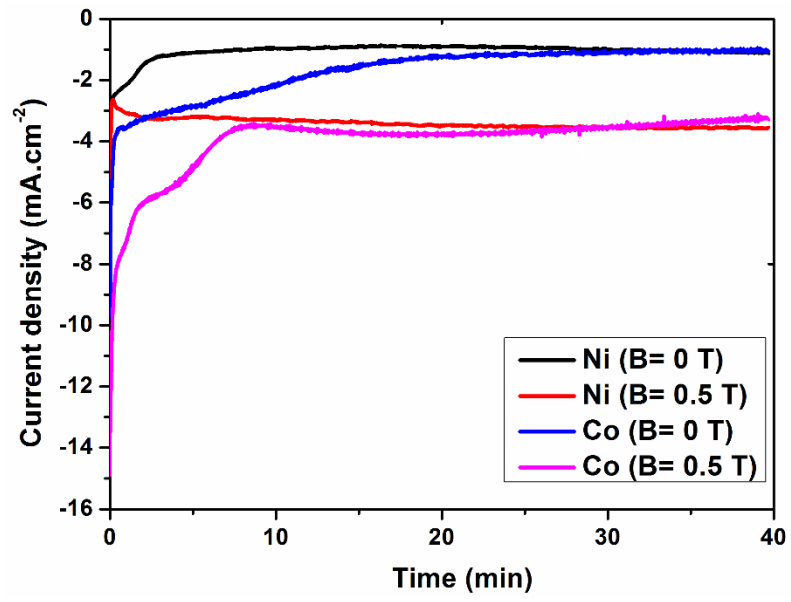


Fig. 5

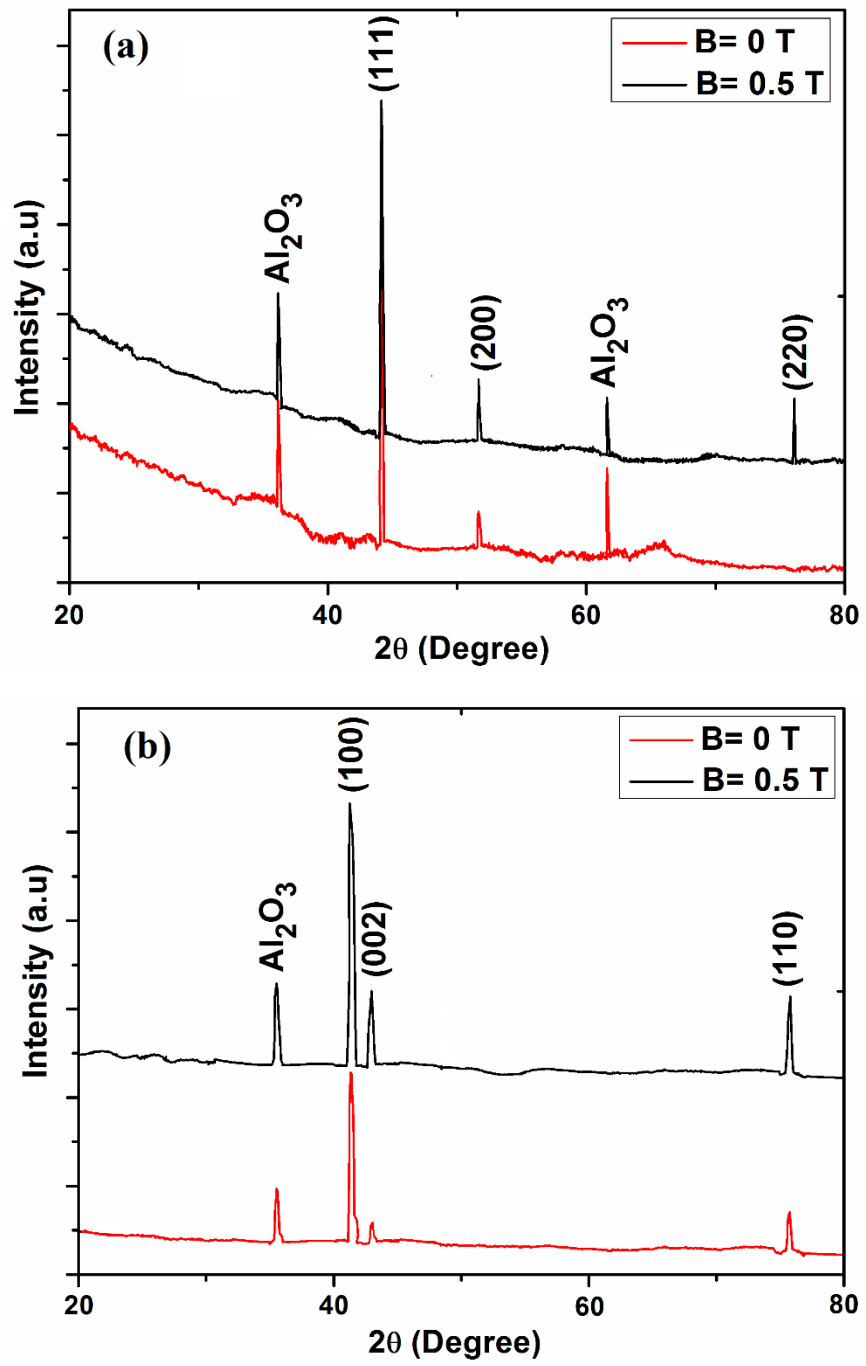


Fig. 6

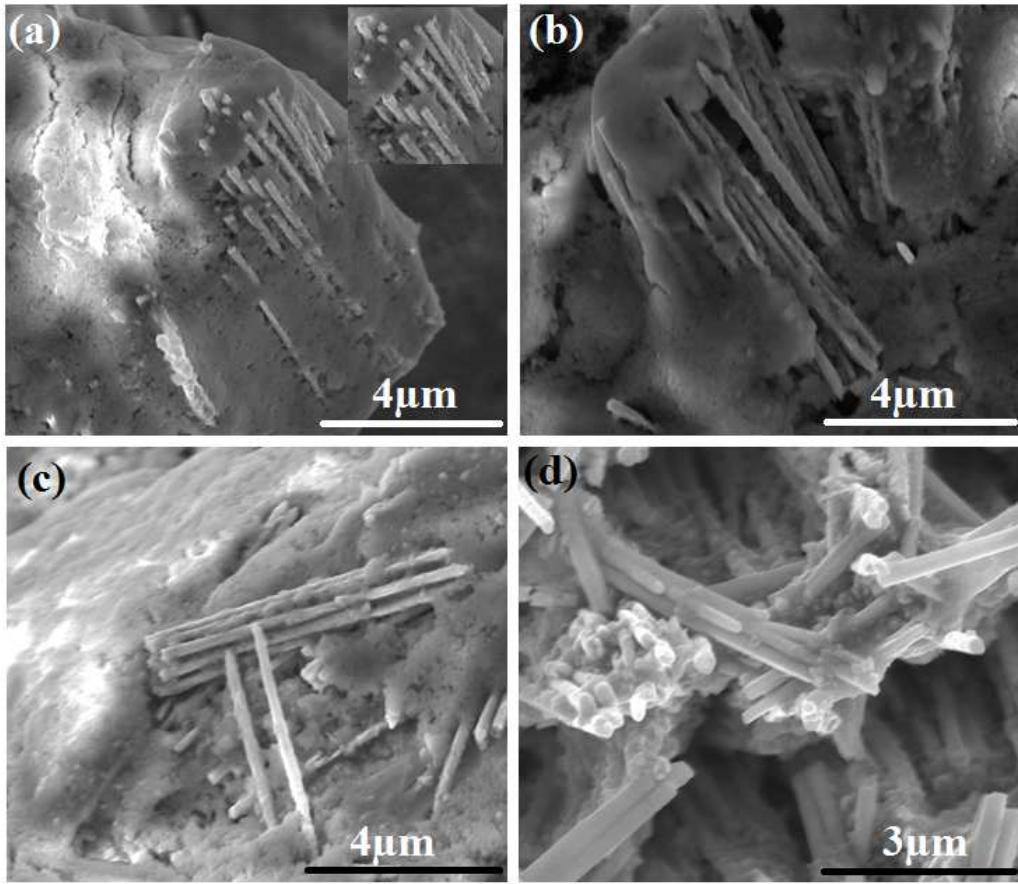


Fig. 7

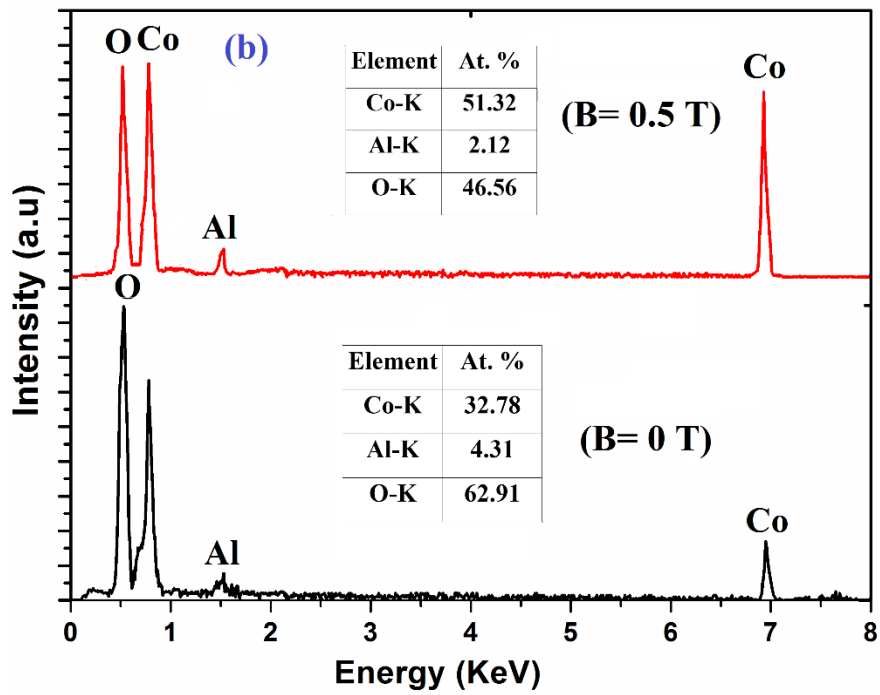
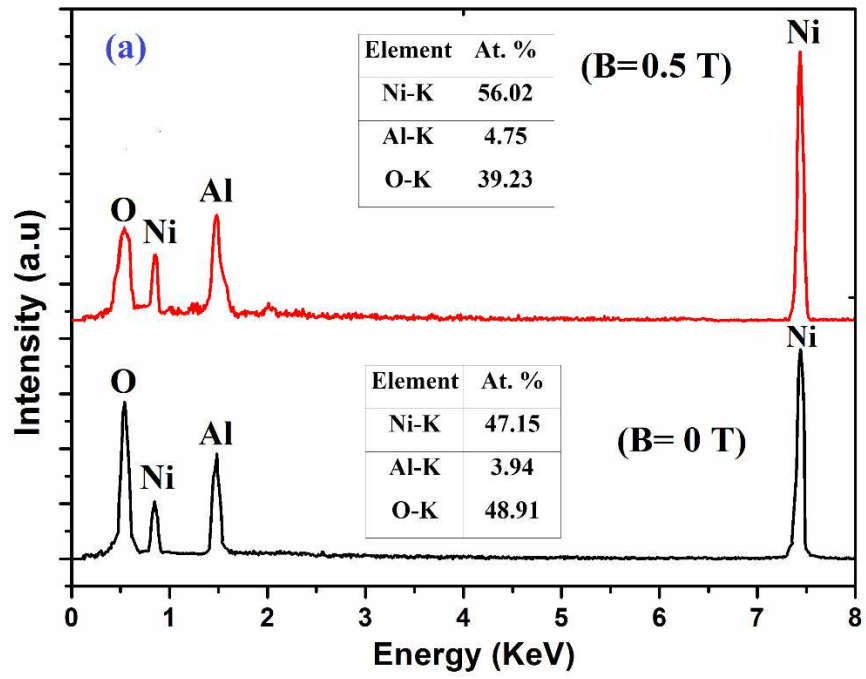


Fig. 8

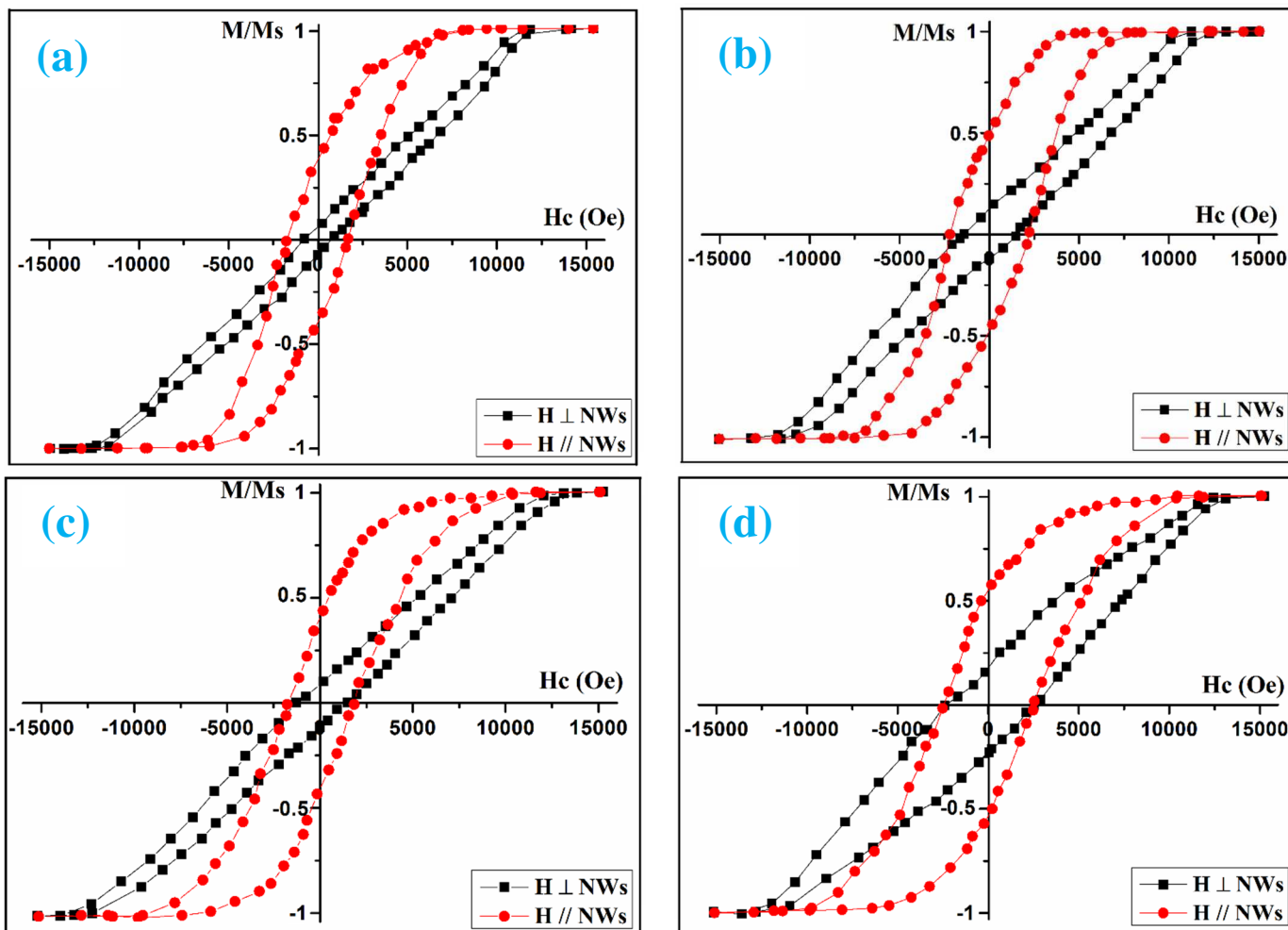


Fig. 9

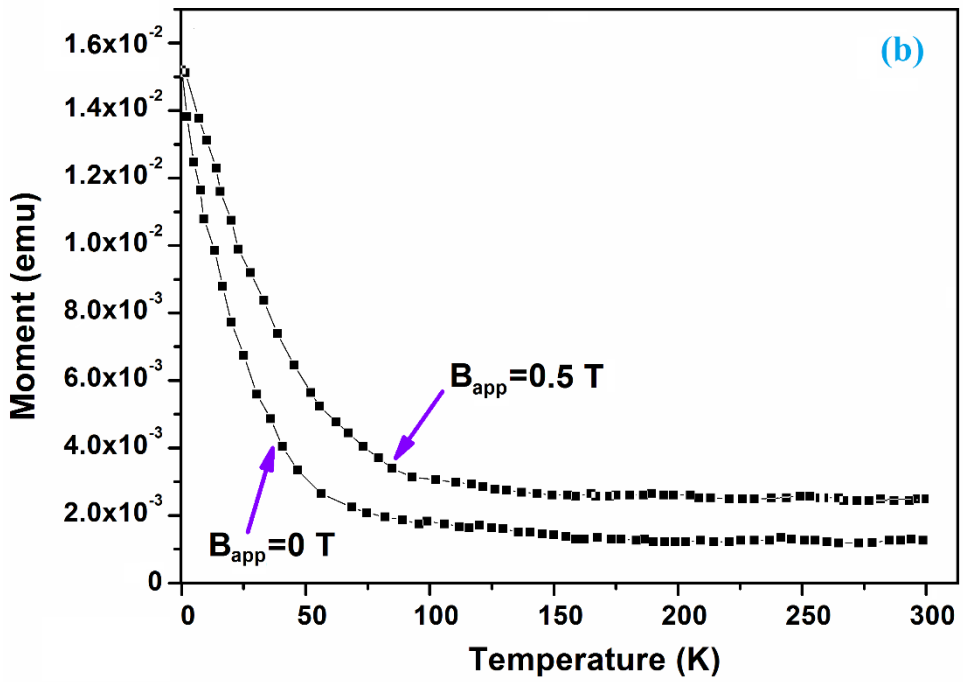
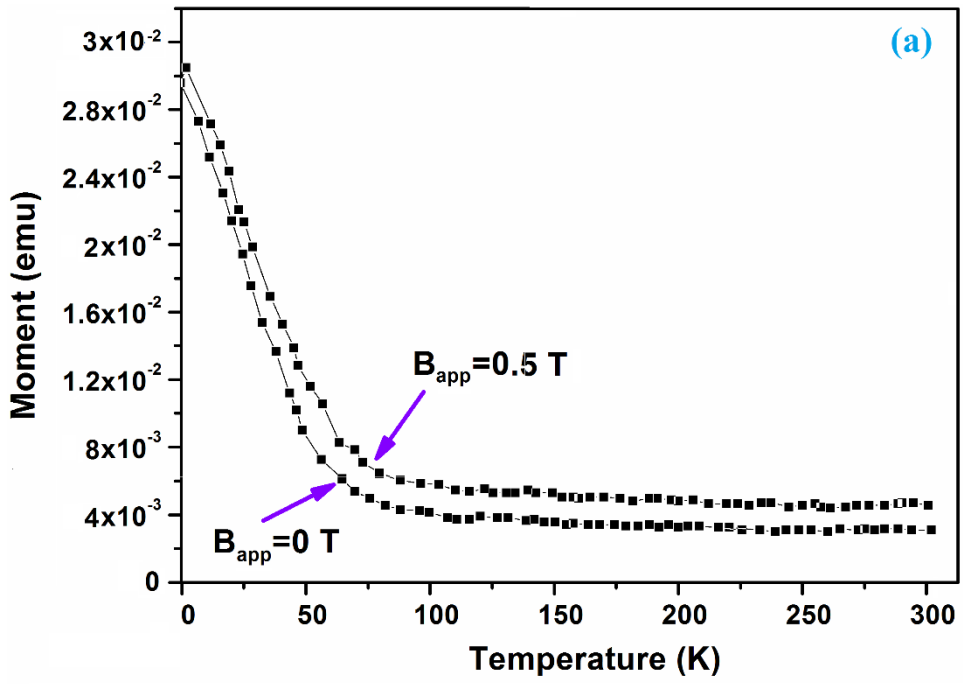
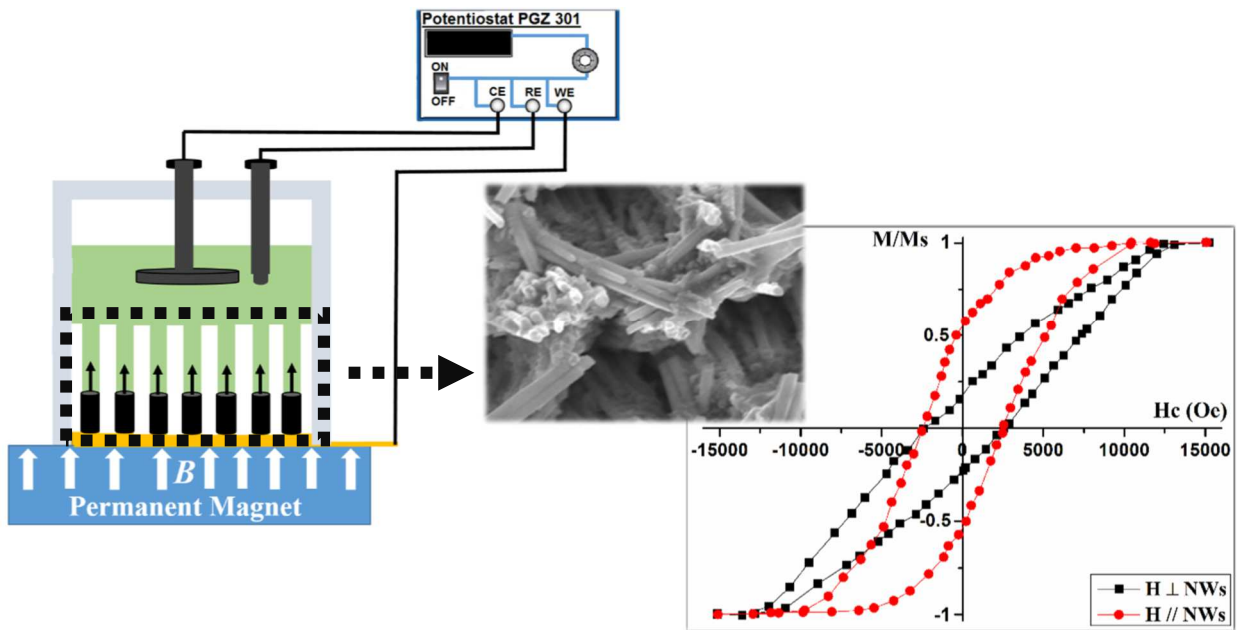


Fig. 10

		H_C^\perp (Oe)	H_C^{\parallel} (Oe)	SQ^\perp	SQ^\parallel
<i>Ni</i> <i>Nanowires</i>	$B_{app} = 0 T$	726	1630	0.066	0.38
	$B_{app} = 0.5 T$	1503	2303	0.13	0.48
<i>Co</i> <i>Nanowires</i>	$B_{app} = 0 T$	1300	1430	0.01	0.43
	$B_{app} = 0.5 T$	2650	2700	0.18	0.51

Table 1. Magnetic parameters of deposited Co and Ni nanowires.



Graphical Abstract